Modal optimization: A steering knuckle case study

Moises Jimenez[*1,2], Guillermo Narvaez[2a], Esau Adame[3b] and Mario Villaseñor[3c]

[1]*Engineering and Science Department, Universidad Iberoamericana Puebla, San Andres Cholula, Puebla, 72810, México*
[2]*Tecnologico de Monterrey, Escuela de Ingeniería y Ciencias, Vía Atlixcáyotl 2301, Reserva Territorial Atlixcáyotl, Puebla, Puebla, 72453, México*
[3]*Technical Development, Volkswagen de Mexico, Km 116 Autopista Mexico-Puebla, 72730, México*

Abstract. A natural frequency optimization of a steering knuckle was performed. It must be strong to support the loads from the road as all the car weight and reactions, in addition to this, it must be designed to prevent resonances with the components around it. The improvements developed for automotive components are evaluated as itself as well as the interaction as a subsystem as well as its interaction in the whole vehicle. We aimed to prevent squeal noise and uncomfortable vibrations between 1 and 3 kHz through optimizing the resonant frequencies of Steering Knuckle and its effect on the components around it as track control arm and disc brake. Optimization was performed modifying the geometry prior to modify the mold. Finite element modal simulations were performed using Ansa, Optistruct and HyperView V14 software. These optimizations were validated with an experimental test using a three-dimensional scanning vibrometer. Results showed that modal optimization can be performed with virtual tools obtaining reliable results.

Keywords: modal analysis; steering knuckle; finite element analysis; noise

1. Introduction

The dynamic of a vehicle corresponds to its translational degree of freedom. Longitudinal dynamic includes acceleration and braking, taking into consideration all of the forces related to driving. Lateral dynamic refers to forces that affect lateral stability. Vertical dynamic includes vertical forces that are tuned through springs and dampers (Heissing and Ersoy 2011). This tuning depends on the stiffness of various components contributing to the dynamic response of a vehicle.

The stiffness contributes to the dynamic response of a vehicle in driving conditions but also contributes in the riding comfort. In driving conditions, different sources induce vibrations to the brake and suspensions systems and in occasions, such induced vibration excites a suspension or

---

∗Corresponding author, Ph.D., E-mail: moises.jimenez@iberopuebla.mx
[a]M.Sc., E-mail: gnarvaezg@itesm.mx
[b]B.Sc., E-mail: esau.adame@vw.com.mx
[c]B.Sc., E-mail: mario.villasenor2@vw.com.mx
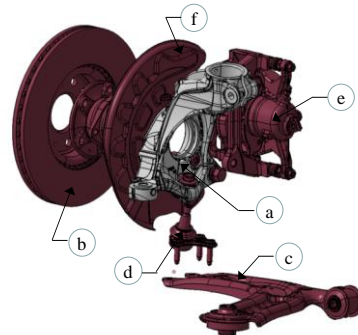
Fig. 1 Suspension subassembly. (a) Steering knuckle, (b) disc brake, (c) track control arm, (d) ball joint, (e) caliper and (f) cover plate

brake component produce undesired vibrations and noises.

To improve passengers comfort as car dynamic performance is necessary to know the behavior of particular components, and if is necessary do some modifications, in order to reduce the noise and the vibration perceived by the passengers, also the optimizations are necessary for new safety or emissions regulations. A common target of manufacturing companies is weight reduction to decrease costs as well as to reach emission regulations.

Weight reduction in suspension components is complex because lightweight materials, such as plastics, composites and magnesium simply do not meet the rigidity, hardness and durability requirements (Lee *et al.* 2017). Such components also have to meet vehicle safety requirements (Cavazzuti *et al.* 2011), every change to meet a requirement or optimization target has an effect in the surrounding components. Automotive components must be evaluated to meet safety, strength and comfort requirements; it is also mandatory to consider the surrounding components.

Evaluation of a component through its modal response is important due to it has an effect on the strength as well as in the comfort, vibrations in a component can be used to detect structural damage through the modal parameter modification due to a change in the natural frequency (Ntakpe *et al.* 2016). To improve passenger comfort based on the noise level in the cabin interior, evaluations such as acoustic modal analysis can be used (Accardo *et al.* 2016). In a vehicle, noise and vibration are the main causes of riding discomfort (Lee *et al.* 2017). Mechanical behavior of chassis components has an influence on the vehicle dynamics and are essential components with the body car in crashworthiness, due to it interchanges the loads from the roads and can generate comfort discomfort. The component that connect the wheels and gives manage the car is the steering knuckle that it also connects the damper, the track control arm and braking components, in Fig. 1 is shown the front axle suspension subassembly.

Steering knuckles must undergo their own safety tests to be released as individual components. However, they must also be evaluated as a subassembly, considering the influence of brake systems. Brake friction induces vibrations and can result in resonance or noise (Iroz *et al.* 2017). The brake system is especially a source of unwanted vibration and noises. Noise in the brake system typically occurs during braking. The most common and annoying problem for brake systems is squeal noise (Dunlap *et al.* 1999).

The range of interest for the high frequency squeal in a disc-brake system is 0-6 kHz. This component can be optimized by improving their torsion, bending and mode frequencies (Cavazzuti *et al.* 2011).
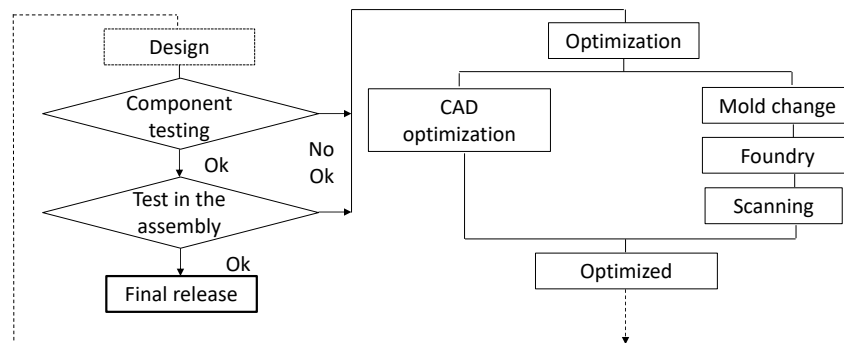
Fig. 2 Process to perform changes in model

Friction induced vibration has been studied by Kapelke *et al*. (2017). In some cases, friction is undesired; however, in automotive systems, friction is desirable in brake systems and friction clutches. Suspension noise is caused when one component excites a suspension component with a natural frequency inside the range of excitation (Xie *et al.* 2014). This noise is typically in the range 200-500 Hz for the rear suspension (Xie *et al.* 2014). Stiffness plays a significant role in noise because it affects the natural frequency of components. Road noise in a vehicle interior is in a mid-frequency range, around 500 Hz for low cruise speeds (Kook *et al.* 2014*)*. Squeal noise is a low-frequency noise defined as being between 1 kHz and 3 kHz (Kim and Zhou 2016).

The geometry can be improved by modifying the mold and evaluating the new part using experimental and Finite Element (FE) analysis. Using computational analysis allows prediction of the natural frequencies prior to fabricating prototypes. Owing to the risk of uncomfortable vibrations and squeal noise, an optimization is performed through modal analysis using commercial software, complemented with experimental analysis.

2. Analysis procedure

To perform the analysis to improve the optimization time, instead of making changes to the three-dimensional Computer-Aided Design model, changes were made to the mold, as described in Fig. 2.

Fig. 3 shows the typical process for a component optimization, design is evaluated as a component if it approves its evaluation of chemical composition, strength, durability and modal response, the component is assembled and tested to evaluate is behavior with the components around it and function tests are performed, if it meets the requirements the design is released, otherwise is optimized. The traditional way is from the Cad is built the Mold and then the components is molten in the foundry, then the component is evaluated, if is necessary the process is do it in a loop until the target is reached. In the proposed process, the mold is directly modified based on analysis and is foundry the component test, if it meets the optimization targets, this is scanned and the CAD model is built from these surfaces, after that is evaluated until it meets the requirements as component as in the assembly.

3. Finite element simulation
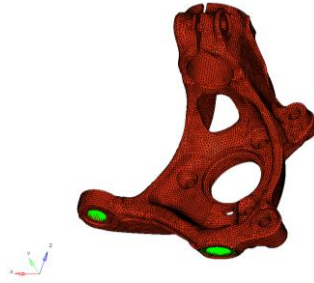
Fig. 3 FEM model Boundary conditions

Table 1 Characteristics of FEM models with different mesh sizes

Mesh Size (mm)	Elements		
	CTETRA	CTRIA	TOTAL
0.5	17,202,552	-	17,202,552
1	14,082,407	588,372	14,670,779
2	1,186,700	94,096	1,280,796
3	355,329	43,652	398,981
4	180,473	12,157	192,630
5	71,915	14,934	86,849
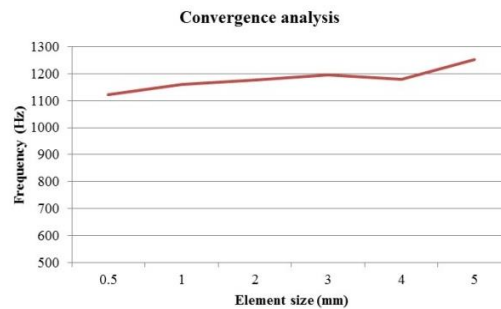
Fig. 4 Convergence analysis

First, a FE modal simulation was performed with the aim of determining the eigenvalues and eigenvectors. Fig. 3 shows the FE model used; spatial constraints are omitted, but these were the same as the experimental test, suspended in air. The FE model was constructed from the original computer-aided design model of the part.

FE models were constructed using solid elements CTETRA and CTRIA. The first-order element characteristics are shown in Table 1. A fine mesh was used because of the complexity of the component.

The software used for the preprocessor was ANSA, the solver was Optistruct and the postprocessor was HyperView. The results were evaluated using convergence analysis to define the mesh size. Mesh element sizes evaluated were 0.5, 1, 2, 3, 4 and 5 mm, as shown in Table 1. The element size used was 2 mm for its rapid convergence and short time to solve the analysis (Fig. 4).

Table 2 Nominal composition in % wt. AlSi7Mg0.3

Si	Mg	Fe	Mn	Ti
10-11.8	0.45	0.19	0.10	0.15

(a) mode 1 at 1125.28 Hz   (b) mode 2 at 1297.5 Hz   (c) mode 3 at 1506.8 Hz

(d) mode 4 at 1975.1 Hz   (e) mode 5 at 2371.7 Hz   (f) mode 6 at 2937.1 Hz
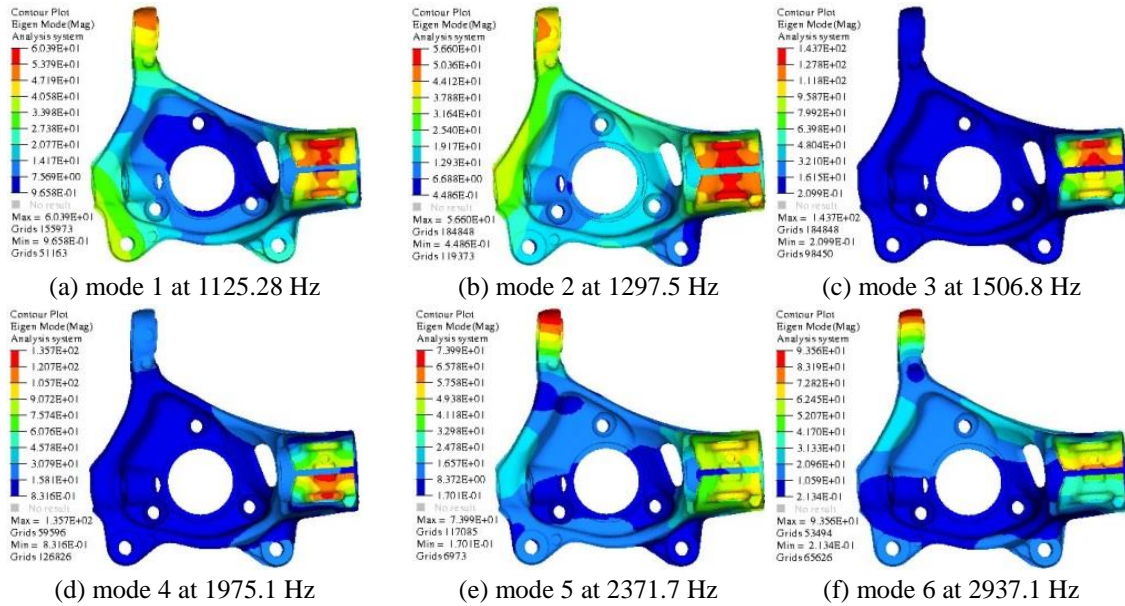
Fig. 5 Eigenfrequency analysis in the initial model of steering knuckle

Table 3 Finite element modal analysis results in the initial model of steering knuckle

|	Wn_1	Wn_2	Wn_3	Wn_4	Wn_5	Wn_6
Hz	1125.28	1297.5	1506.8	1975.1	2371.7	2937.1

(a) Frontal view   (b) Rear view
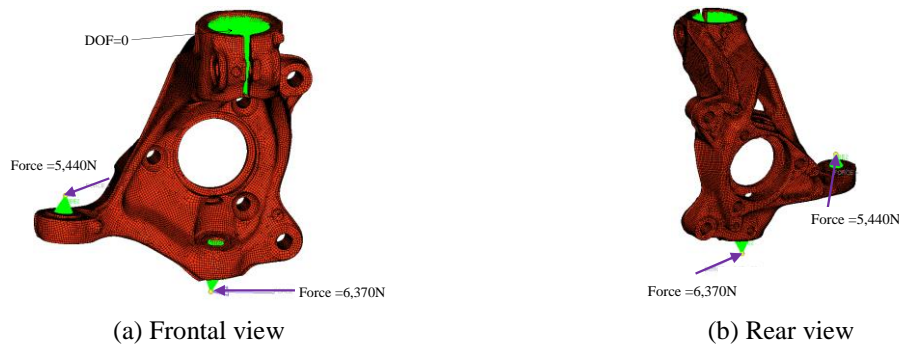
Fig. 6 Boundary condition and spatial constraint for the static analysis

Young's modulus E=74,000 N/mm^2 and Poisson's ratio v=0.33, density ρ=2.7e-9 tonne/mm^3. Table 2 shows the composition of AlSi11 part (DIN 2013).

Eigenvectors of the finite element analysis are shown in Fig. 5, in Table 3 are shown the eigenvalues.

(a) Frontal view   (b) Rear view
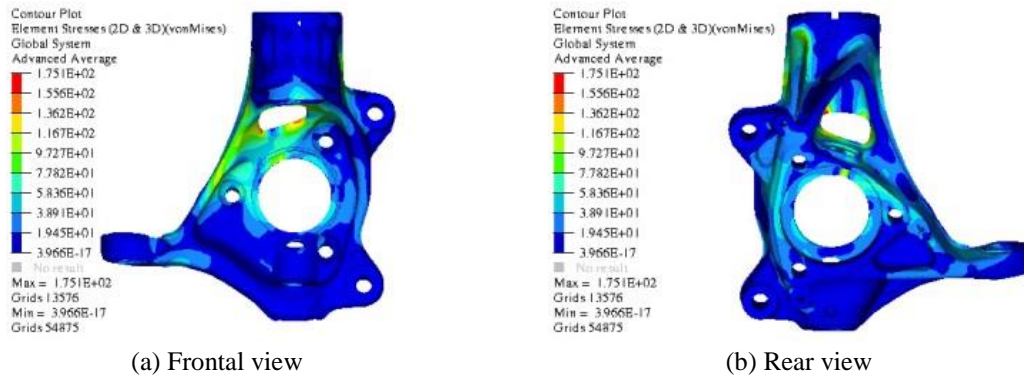
Fig. 7 Stress results for the static analysis

(a) Frontal view   (b) Rear view

Fig. 8 Model comparation

(a) Cloud points   (b) Detail
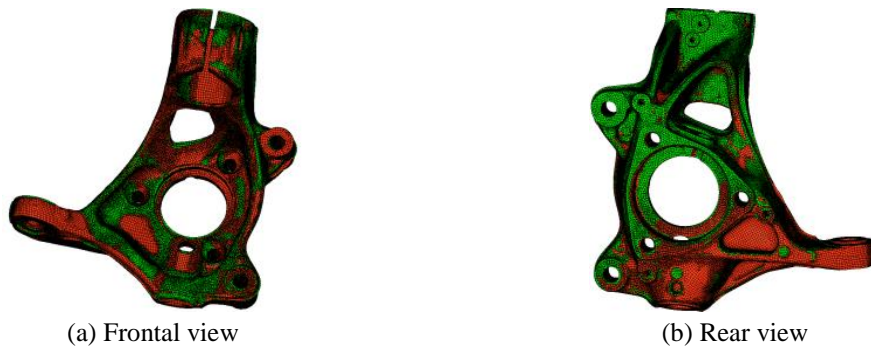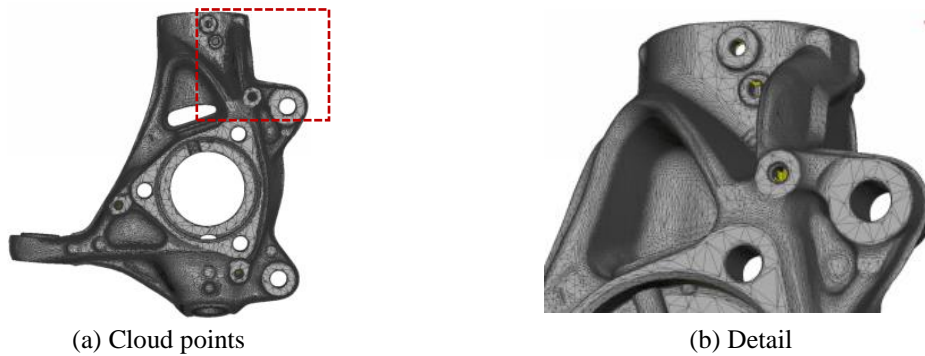
Fig. 9 Scanning

Under the assumption that stiffness has a direct effect on the modal response, a static analysis was performed. The load case was simplified using spatial constraint of 6DOF=0 (Degrees of freedom) on the area of the contact of the damper. A load of 6,370 N was applied on the center of the ball joint that connects the track control arm to represent brake force. A load of 5,440 N was applied on the ball joint position that connects the rod from the steering box with the steering knuckle to represent rotation of the tire, as it is shown in Fig. 6. The Von Mises stress results are shown in Fig. 7.

Table 4 Finite element modal analysis results in the proposed model of Steering Knuckle

	Wn$_1$	Wn$_2$	Wn$_3$	Wn$_4$	Wn$_5$	Wn$_6$
Hz	1143.7	1323.2	1582.6	2057.9	2376	2938.9

Fig. 10 Experimental set up for steering knuckle

(a) mode 1 at 1103.5Hz (b) mode 2 at 1301 Hz (c) mode 3 at 1526 Hz

(d) mode 4 at 1971 Hz (e) mode 5 at 2322 Hz (f) mode 6 at 2872 Hz
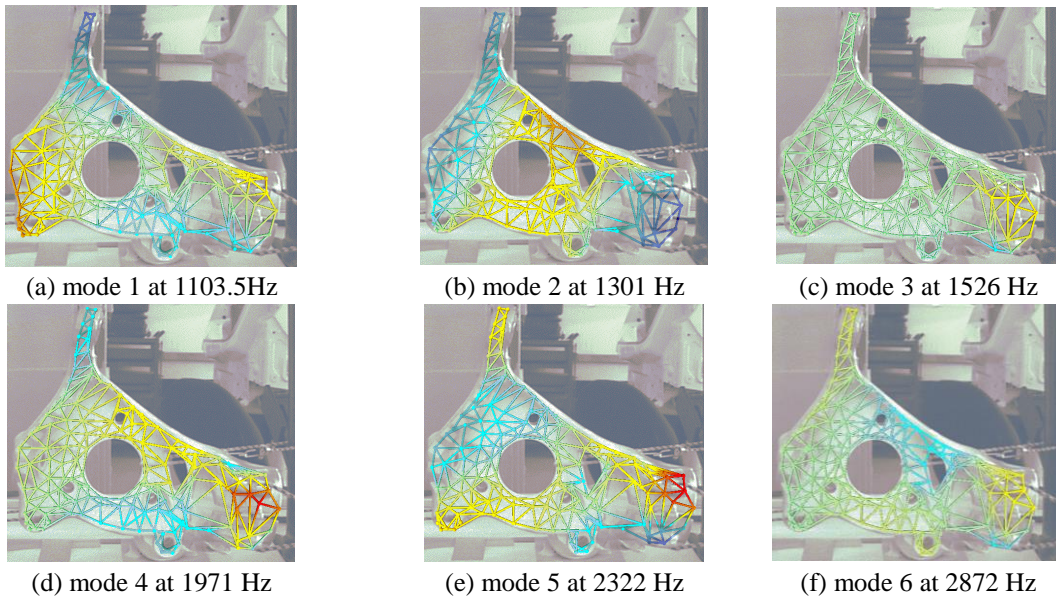
Fig. 11 Eigenfrequency analysis in the initial model of steering knuckle

Table 5 Experimental results in steering knuckle modal analysis

	Wn$_1$	Wn$_2$	Wn$_3$	Wn$_4$	Wn$_5$	Wn$_6$
Ave(Hz)	1103.5	1301	1526	1971	2322	2872
Min(Hz)	1094	1292	1512	1962	2307	2855
Max(Hz)	1114	1310	1534	1993	2341	2898
Δ(Hz)	20	18	22	31	34	43
Error(%)	1.81	1.38	1.44	1.57	1.46	1.5

Based on these results modifications were made to optimize the steering knuckle design. Fig. 8 shows the areas where the thickness of the material was increased based on the stress results in
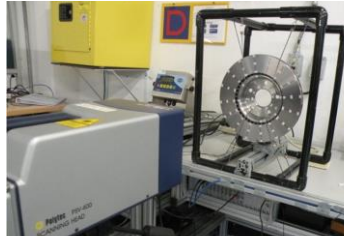
Fig. 12 Experimental set up, for the disc brake measurement

Table 6 Experimental results in the modal analysis of the disc brake

	Wn_1	Wn_2	Wn_3	Wn_4
Ave(Hz)	979	2276	3700	5179
Min(Hz)	968	2248	3648	5096
Max(Hz)	992	2304	3744	5264
Δ(Hz)	24	56	96	168
Error(%)	2.45	2.26	2.59	3.24

Fig. 13 FE model of the track control arm

Fig. 7, the original design is in orange and the changes are on green. After modifying the mold, the newly formed parts were scanned, as shown in Fig. 9.

The scanned modified part was imported as a FE model in STL format. The mesh model was repaired and the final FE model was built with element size 2 mm. The model was constructed using 830,755 CTETRA elements and 42,100 CPYRA for a total of 872,855 solid elements of the first order. The eigenvectors result of this simulation are similar to those of the original model. Changes to the eigenvalues are shown in Table 4.

4. Experimental analysis

A non-contact scanning vibrometer (Polytec) was used because it can eliminate the effect of accelerometer mass (Marwitz and Saber 2016). Fig. 10 shows the experimental set up.

Fig. 11 shows the experimental results in wireframe. Table 5 shows a summary of the experimental results. The excitations were performed on the two points where the caliper was fixed to 22 specimens.

Table 7 Results of track control arm finite element modal analysis

	Wn_1	Wn_2	Wn_3	Wn_4	Wn_5	Wn_6	Wn_7	Wn_8
Hz	217.5	272.4	448.8	709	822	895.5	1047.2	1220.7
	Wn_9	Wn_{10}	Wn_{11}	Wn_{12}	Wn_{12}	Wn_{14}	Wn_{15}	Wn_{16}
Hz	1450.1	1675.1	1852	1933.4	2054.1	2117.9	2215.2	2273.4
	Wn_{17}	Wn_{18}	Wn_{19}	Wn_{20}				
Hz	2300.3	2531.8	2620.7	2820.3				

(a) mode 7 at 1047.2Hz (b) mode 8 at 1220.7 Hz (c) mode 9 at 1450.1 Hz

(d) mode 11 at 1852 Hz (e) mode 12 at 1933.4Hz (f) mode 15 at 2215.2 Hz

(g) mode 16 at 2273.4Hz (h) mode 20 at 2820.3Hz
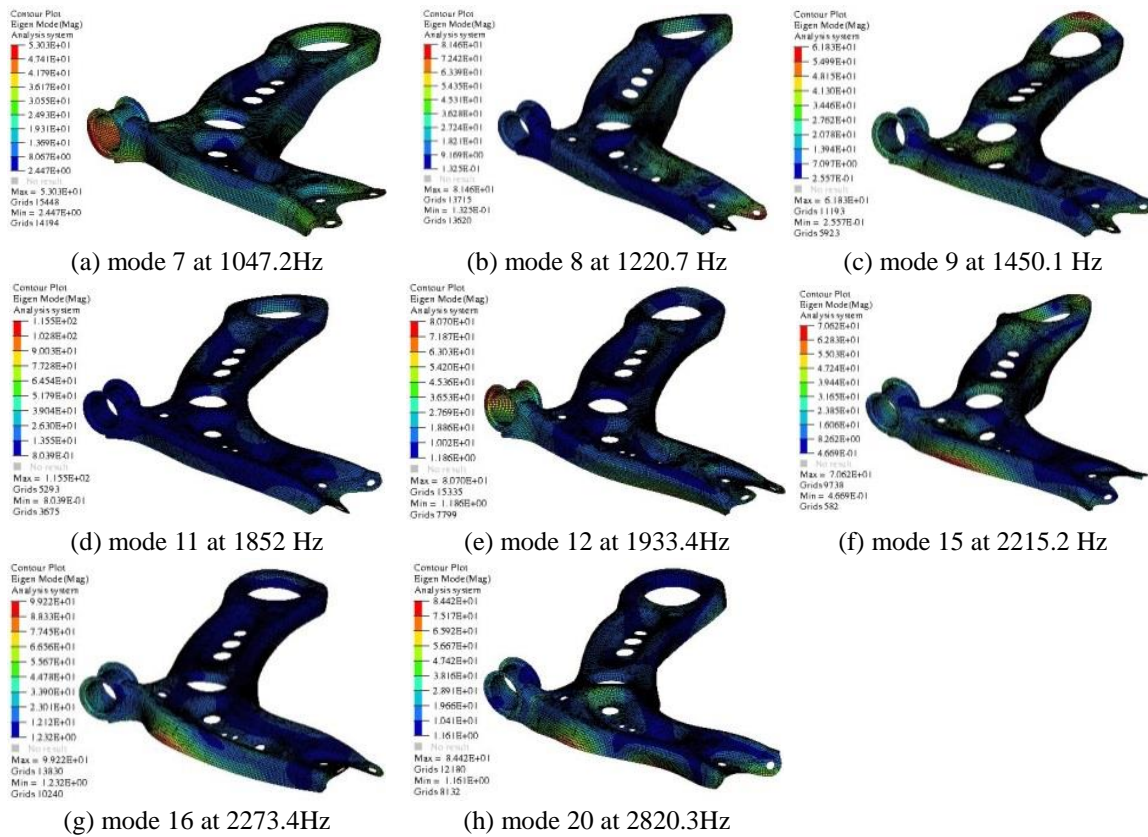
Fig. 14 Eigenvectors for finite element track control arm

The eigenvalues of the disc brake are known. Fig. 12 shows the experimental set up. Table 6, shows the first four natural frequencies measured in 40 specimens.

The subassembly is composed of the steering knuckle, the disc brake and the track control arm (Fig. 1). To understand the effect of the track control arm in this assembly, a FE simulation was performed. The track control is a sheet metal component, based on this the FE model was built using 2D shell element with 15,440 elements, 14,800 CQUAD, 789 TRIA. To simulate welds, 43 rigid elements are used to join the hub and the shell, as shown in Fig. 13. The mechanical properties for typical steel were used: E=210,000 N/mm^2, ν=0.3, ρ=7.85e-9 tonne/mm^3.

Table 7 shows the results in the range 0-3 kHz. Fig. 15 shows the eigenvectors in the range of
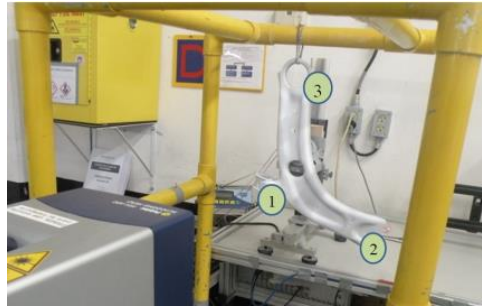
Fig. 15 Experimental set up, for track control arm

Table 8 Experimental results in track control arm

	Wn$_2$	Wn$_3$	Wn$_4$	Wn$_5$	Wn$_6$	Wn$_7$	Wn$_8$	Wn$_{10}$
Ave(Hz)	254.67	428	629.3	848	980	1063	1296.3	1610
Min(Hz)	247	428	621	847	976	1062	1289	1606
Max(Hz)	285	428	636	849	985	1064	1304	1613
Δ(Hz)	38	0	15	2	9	2	15	7
Error(%)	14.9	0	2.38	0.24	0.92	0.19	1.16	0.43
	Wn$_{11}$	Wn$_{13}$	Wn$_{15}$	Wn$_{16}$	Wn$_{17}$	Wn$_{18}$	Wn$_{19}$	Wn$_{21}$
Ave(Hz)	1809	2029.7	2204	2285.7	2358.3	2569	2786.7	2971
Min(Hz)	1766	2022	2204	2271	2344	2563	2777	2960
Max(Hz)	1832	2038	2205	2300	2373	2578	2797	2982
Δ(Hz)	66	16	1	29	29	15	20	22
Error(%)	3.65	0.79	0.05	1.26	1.22	0.58	0.71	0.74

interest for noise prevention (1-3 kHz).

Fig. 15 shows the three excitation points used. For each excitation point, measurement was taken for 20 components from the same production lot. This excitation pattern corresponds to the kinematic points of the track control arm points 1 and 2 with the subframe points the ball joint that connect it to steering knuckle. Table 8 summarizes the main experimental results of the measurement.

5. Results and discussion

To verify the prediction reliability of the FE simulation, these results were compared with experimental results in the range of interest for noise prevention (1-3 kHz), Table 9 shows the evaluation for the steering knuckle. Table 10 shows the evaluation for the track control arm.

The maximum error between experimental and FE results is 4.4% for the steering knuckle and 5.8% for the track control arm. The error in experimental results are evaluating with the difference of the maximum and minimum value reported (Δ) and compared with the average (Ave), the error is 1.81 for the Steering knuckle and 14.9% for the track control arm as it is shown in Tables 5 and 8 respectively, based on this is believed that FE results have good confidence.

Table 9 Experimental results Vs FEA responses in steering knuckle

	Wn_1	Wn_2	Wn_3	Wn_4	Wn_5	Wn_6
Measure(Hz)	1103.5	1301	1526	1971	2322	2872
FEA(Hz)	1143.7	1323.2	1582.6	2057.9	2376	2928.5
Δ(Hz)	40.2	22.2	56.6	86.9	54	56.5
Error(%)	3.64	1.71	3.71	4.41	2.33	1.97

Table 10 Evaluation of the natural frequencies in track control arm

	Wn_7	Wn_8	Wn_{10}	Wn_{11}	Wn_{13}	Wn_{15}	Wn_{16}	Wn_{17}	Wn_{18}	Wn_{19}	Wn_{21}
Exp(Hz)	1063	1296.3	1610	1809	2029.7	2204.5	2285.7	2358.3	2569	2786.7	2971
FEA(Hz)	1047.2	1220.7	1675.1	1852	2054.1	2215.2	2273.4	2300.3	2531.8	2820.3	2924.4
Δ(Hz)	15.8	75.6	65.1	43	24.43	10.7	12.3	58.3	37.2	33.63	46.6
Error(%)	1.49	5.83	4.04	2.38	1.2	0.49	0.54	2.47	1.45	1.21	1.57

Table 11 Natural Frequencies in the range of interest

TCA	Wn_7	Wn_8	Wn_9	Wn_{10}	Wn_{11}	Wn_{12}	Wn_{13}	Wn_{14}	Wn_{15}	Wn_{16}	Wn_{17}	Wn_{18}	Wn_{19}	Wn_{20}	Wn_{21}
	1063	1296	1450	1610	1809	1933	2030	2118	2204	2286	2358	2569	2787	2820	2971
DB										Wn_2					
										2276					
SK	Wn_1	Wn_2	Wn_3			Wn_4				Wn_5			Wn_6		
I	1125	1297	1507			1975				2372					2937
p	1104	1301	1526			1971				2322			2872		

The track control arm and disc brake have natural frequencies above and below those summarized in Table 9. However, the present work is focused on the range of interest, and how this range influences the other components.

For the disc brake, only the experimental results are considered. To compare the natural frequencies Table 11 summarized the results not seen in the experimental analysis, evaluating in these frequencies the FE results, where TCA is track control arm, DB is disc brake and SK is steering knuckle. The natural frequencies 9, 12 and 14 for the track control arm were found using the FE simulation. These were not identified it in the experimental work. Because the steering knuckle has 15 natural frequencies in the range of interest, these are compared with the disc brake as well as initial (i) and proposed (p) steering knuckle designs

None of the natural frequencies are similar; therefore, the final model was improved to eliminate the resonances between the eighth natural frequency of the track control arm and the second natural frequency of the steering knuckle.

The weight was modified from 2.44687e-3 tonne in the original model to 2.35227e-3 tonne in the improved model.

6. Conclusions

A modal optimization was performed using FE simulation to prevent noise and undesirable

vibrations. Results were validated with experimental results using a three-dimensional scanner and a vibrometer, taking into account the modal responses of the disc brake and the track control arm. Through static analysis, changes to the geometry of the steering knuckle were proposed, to modify the modal response based on it stiffness. The geometry was modified directly using a mold and tested after casting a new component.

The FE analysis results and experimental results show good agreement. The advantage of FE simulation over the experimental results is that with one simulation all the natural frequencies are found, whereas with experimental results is necessary to excite the components in different positions to find all the natural frequencies. Although the track control arm was excited at three kinematic points and samples were tested for each excitation point, natural frequencies 1, 9, 12 and 14 were not found.

Squeal noise and uncomfortable vibrations can be prevented by performing modal analysis; however, it is necessary to analyze components in the vicinity, not only the component of interest.

The most critical component in this subassembly is the track control arm because it has natural frequencies in the range of interest. Although improvements to the eighth natural frequency of the track control arm and the second natural frequency of the steering knuckle is 5 Hz is not possible to increase the difference for the fact that seventieth natural frequency of the track control arm and the first of the steering knuckle tend to converge, for this is not possible to improve it more for the manufacturing constraints of the assembly and the spatial constraints of the components for the kinematics suspension.

Errors found in the experimental results are greater in the track control arm than those in the steering knuckle. The track control arm is manufactured using two main processes, stamping and welding. In contrast, the steering knuckle is manufactured using a casting process.

Acknowledgments

References

Accardo, G., Chiariotti, P., Cornells, B., El-Kafafy, M., Peeters, B., Janssens, K. and Martanelli, M. (2016), "Experimental acoustic modal analysis of an automotive cabin challenges and solutions", *J. Phys.: Conf. Ser.*, **1075**(1), 012026.

Cavazzuti, M., Baldini, A., Bertocchi, E., Costi, D., Torriceli, E. and Moruzzi, P. (2011), "High performance automotive chassis design: A topology optimization based approach", *Struct. Multidisc. Optim.*, **44**(1), 45-56.

DIN EN 1706 (2013), *Aluminium and Aluminium Alloys-Castings-Chemical Composition and Mechanical Properties*.

Dunlap, K.B., Riehle, M.A. and Longhouse, R.E. (1999), "An investigative overview of automobile disc brake noise", *SAE Trans.*, 515-522.

Heissing, B. and Ersoy, M. (2011), *Chassis Handbook*, Vieweg + Teubner Verlag, Springer.

Iroz, I., Hans, M. and Eberhard, P. (2017), "Transient simulation of friction-induced vibrations using an elastic multibody approach", *Multibod. Syst. Dyn.*, **39**(1-2), 37-39.

Kapelke, S., Seemann, W. and Hetzler, H. (2017), "The effect of longitudinal high-frequency in plane vibrations on a 1-DOF friction oscillator with compliant contact", *Nonlin. Dyn.*, **88**(4), 3003-3015.

Kim, C. and Zhou, K. (2016), "Analysis of Automotive disc brake squeal considering damping and design modifications for pads and a disc", *Int. J. Automot. Technol.*, **17**(2), 213-223.

Kook, H.S., Lee, D. and Ih, K.D. (2014), "Vehicle interior noise model based on a power law", *Int. J. Automot. Technol.*, **12**(5), 777-785.

Lee, K.H., Bak, J.H., Park, J.L. and Lee, C.H. (2017), "Vibration reduction of H/shaft using electromagnetic damper with mode change", *Int. J. Automot. Technol.*, **18**(2), 255-261.

Marwitz, S. and Zabel, V. (2016), "Operational modal analysis with a 3D laser vibrometer without external reference", *Rotat. Mach. Hybr. Test Meth. Vibro-Acoust. Las. Vibrometr.*, **8**, 75-85.

Ntakpe, J.L., Gillich, G.R., Mitultu, I.C., Praisach, Z.I. and Gillich, N. (2016), "An accurate frequency estimation algorithm with application in modal analysis", *Roman. J. Acoust. Vibr.*, **13**(2), 98-103.

Xie, M.S., Zhang, G.R., Li, J.H. and Fritsch, R. (2014), "Brake pad taper wear on brake moan noise", *Int. J. Automot. Technol.*, **15**(4), 565-571.

CC